Catal Lett (2013) 143:1285–1293
DOI 10.1007/s10562-013-1066-7

A New Deactivation Mechanism of Sulfate-Promoted Iron Oxide

Wenping Shi · Jianwei Li

Received: 28 April 2013 / Accepted: 3 July 2013 / Published online: 26 July 2013

Abstract The deactivation of sulfate-promoted iron oxide in the esterification of acetic acid and *n*-butanol was studied. The sulfate-promoted iron oxide was used ten runs and 10 h, continually and accumulatively. After ten-run continual use of the catalyst, a considerable deactivation happened to it. The fresh and the deactivated catalysts were compared by means of many characteristic methods including FTIR, XRD, BET, SEM, TG–DSC, and NH_3–TPD, to disclose some possible reasons for the deactivation of sulfate-promoted iron oxide in the esterification. Based on the comparative analyses of IR patterns of the fresh catalyst and the deactivated one, a deactivation mechanism is tentatively proposed. Namely, surface sulfate groups, which are originally coordinated to Fe^{3+} cations and can so induce and generate strong Lewis acidity of Fe^{3+} cations, may have been gradually turned into free sulfate groups and sulfate esters arisen from strong Lewis-acidic Fe^{3+} cations' being hydrolyzed by H_2O and their being alcoholyzed by *n*-butanol, which leads to a gradual destruction of the originally strong coordination between Fe^{3+} cations and surface sulfate groups, so leading to the acidity degradation of the catalyst, and so finally leading to the deactivation of it. Emphatically, in the proposed mechanism, the water produced from the esterification may play a key role on the deactivation of the catalyst, because it can directly hydrolyze some strong Lewis-acidic Fe^{3+} cations of the catalyst and indirectly promote the alcoholysis of them, to form weak Lewis-acidic Fe–OH species. The deactivated catalyst has a larger crystallinity, a smaller specific surface area, a smaller sulfate groups content, a weaker acidity than the fresh. All these phenomena, accompanying the deactivation of sulfate-promoted iron oxide, can be interpreted by the proposed deactivation mechanism very well.

Keywords Solid acid · Sulfate-promoted iron oxide · Deactivation · Esterification

W. Shi (✉) · J. Li
State Key Laboratory of Chemical Resource Engineering,
Beijing University of Chemical Technology,
Beijing 100029, China
e-mail: gaigeguanyin@126.com

1 Introduction

Up to now, there are still a lot of liquid acid catalysts which are extensively used in chemical industry, which are accompanied by a lot of problems such as corrosions, pollutions and unwanted side reactions and so on. People are trying to replace them with solid acids. Among the solid acids, the sulfate-promoted metal oxides have been attracting more and more attention in recent years [1–7] due to their unique advantages over those traditional liquid acid catalysts. For example, they are quite stable to moisture, air, and heat, and they are also less corrosive to reactors and containers, and they are also environmentally friendly [8–13]. Above all, they exhibit extremely high initial activities in catalyzing many organic reactions such as esterification, isomerization of *n*-alkanes, cracking reaction, and so forth, even at very mild conditions [2–5, 9–13]. However, there is a fatal problem for people to utilize them as practical catalysts in chemical industry to replace those liquid acid catalysts with them. The problem is that sulfate-promoted metal oxides often rapidly deactivate despite of their initial high activities [1]. Thus, there appeared a lot of methods used to modify them to deal with the puzzle. For example, sol–gel preparing routes [14] can usually give them larger specific surface areas than

traditional precipitation preparing routes, which generally means there can obtain more active sites on the catalysts prepared by sol–gel routes than by precipitation routes so as to improve their stabilities and retard their deactivation. Besides, doping other aided elements to the bulks of sulfated metal oxides can also retard their deactivation to some extent [15, 16]. However, these modifying methods are not enough to solve the problem. It is obviously important for researchers to find the exact reasons for the deactivation of the catalysts, to pave the way for solving the problem. Many deactivation researches were focused on sulfate-promoted zirconia in alkane reactions [17, 18]. There put out some possible reasons for the deactivation of sulfate-promoted zirconia [17], such as acidity degradation, coke formation, sulfur loss, phase transformation, and so on. However, up to date, there are still a lot of disputes and obscurities on the exact reasons for the deactivation of sulfate-promoted metal oxides especially in other reactions, e.g., esterification, than alkane reactions. The paper attempts to clarify some possible reasons for their deactivation in the esterification of acetic acid and *n*-butanol by studying the fresh and deactivated sulfate-promoted iron oxides by means of many characteristic methods.

2 Experiments

2.1 Materials

Chemicals used in the present work, such as iron(III) chloride hexahydrate ($FeCl_3{\cdot}6H_2O$), ammonia (25 % $NH_3{\cdot}H_2O$), anhydrous ethanol (C_2H_5OH), concentrated sulfuric acid (98 % H_2SO_4), *n*-butanol ($C_4H_9O_{10}$), and glacial acetic acid (CH_3COOH), all analytical reagent grade, were purchased from SCRC of China.

2.2 Preparations of the Catalysts

70 g $FeCl_3{\cdot}6H_2O$ was dissolved in deionized water (250 ml) in an ice-water bath, followed by adding aqueous ammonia to the solution with stirring, until the final pH of the solution was adjusted to 8–9. The obtained precipitate was kept and aged in the mother liquid for 12 h at room temperature. The aged precipitate was filtered in a Buchner funnel and washed with deionized water until there was no Cl^- detectable by $AgNO_3$ (0.1 M) in the last-patch water solution filtered out of the Buchner funnel. The washed precipitate was dried at 373 K for 12 h, and the dried hydroxide was ground and sieved by a 100-mesh sieve. Subsequently, the sieved hydroxide was then sulfated for 24 h by adding H_2SO_4 (0.5 mol/l) on the ratio of 15 ml solution to 1 g hydroxide. Further, the obtained mixture was filtered and the filter cake was dried at 373 K for 12 h and sieved by a 100-mesh sieve. Finally, the sample was calcined at 773 K for 3 h in static air atmosphere to obtain the sulfate-promoted iron oxide.

2.3 Deactivation Phenomena of Sulfate-Promoted Iron Oxide

The *n*-butanol and acetic acid esterification was used as a model reaction to evaluate the catalytic activities and stabilities of the prepared sulfate-promoted iron oxide samples. The reaction was performed at atmospheric pressure in a three-neck flask, which was equipped with a condenser and a water separator and heated by a temperature-controlled oil-bathed pot. The ratio of acetic acid to *n*-butanol is 20:50 ml (0.3494:0.5462 mol), and the catalyst amount (m_{cat}) was 3 g.

The detailed experimental strategies were as follows: (1) the reactant system was firstly heated up to the refluxing temperature (98–112 °C) and reacted for 1 h; (2) when the reaction ended, the liquid product was distilled out of the reaction system until the temperature of the reaction system reached to 116 °C and there seemed to be little liquid remains on the left catalyst, and the corresponding condensed liquid product was analyzed by the gas chromatography; (3) the catalyst, still kept in the flask without any further processing, was continued to be used for the next-cycle esterification by adding a new reaction mixture of the acetic acid (20 ml) and *n*-butanol (50 ml). The new and deactivated sulfate-promoted iron oxides are denoted as Fe0 (the fresh catalyst before deactivation) and Fe10 (the deactivated one after deactivation), respectively.

The used gas chromatography is SP-6890 (ShanDongLuNanRuiHong Chemical Instrument Corporation) equipped with a capillary chromatographic column of FFTP (50 m × 0.32 m × 1 μm). The FID detector is used, and the column temperature is 80 °C and the injection temperature is 180 °C.

2.4 Characterization of the Catalysts

Fourier transform infrared spectroscopy (FTIR) method was used to acquire the transmission modes of sulfate-promoted iron oxide samples on a Bruker TENSOR 27 FT-IR spectrometer with a MCT detector. The samples were mixed with KBr and compacted into thin pellets under 8 kPa. The spectra in the range of 4,000–600 cm^{-1} were recorded at room temperature.

X-ray diffraction (XRD) patterns were recorded on a Brucker D8 diffractometer, with a copper tube as radiation source ($\lambda = 0.15405$ nm), and operated at 40 kV and 20 mA. The XRD profiles were recorded at 1° (2θ) per minute. The scan range was from $2\theta = 10$–80°.

The specific surface areas of the solids were measured via a Sorptomatic 1990 instrument (Thermo Electron) through nitrogen adsorption/desorption at 77 K and were calculated by the Brunauer–Emmett–Teller (BET) method. Micropore volume was obtained by using t-plot method as well as the pore size distribution of the solids was determined according to the BJH method.

The scanning electron microscope (SEM) was performed on an SUPRA^{TM} 55 (produced by IEISS) apparatus at 20 kV.

The thermo gravimetric analysis (TG) was performed on an STA409PC apparatus, in which the heating rate was 10 °C/min from room temperature to 1,000 °C and under the atmosphere of high-purity Ar (30 ml/min). For each experiment, ~13.0 mg of sample was used.

Temperature programmed NH_3 desorption (NH_3–TPD) was performed on CHEMBET-3000 (American Quantachrome Company) equipped with a TCD detector. The sample of ~0.2 g catalyst was treated at 400 °C for 1 h in helium (20 ml/min) prior to the NH_3 adsorption at 100 °C. After the sample was purged for 30 min by helium (20 ml/min), the TPD spectra were recorded at a heating rate of 10 °C/min from 100 to 600 °C.

3 Results and Discussion

3.1 Deactivation Phenomena of Sulfate-Promoted Iron Oxide

The stability of sulfate-promoted iron oxide is shown in Fig. 1. Sulfate-promoted iron oxide was used ten runs and 10 h, continually and accumulatively. The catalyst obtains an initial catalytic activity of 84.48 %. The second-run activity of 94.60 % is the largest in all the runs. However, from the third-cycle on, the catalytic activity of the catalyst steeply drops and the last-run activity is only 51.48 %, indicating a considerable deactivation of the catalyst after the continual use of it. The paper will try to find the reasons for the deactivation of it by some characteristic methods as below.

3.2 FT-IR Patterns of the Catalysts

FT-IR patterns of the fresh and the deactivated sulfate-promoted iron oxides are given in Figs. 2, 3.

The broad band at 3,423 cm^{-1} is the stretching vibrating adsorption band of the O–H bond in the surfaced hydroxyl and in the planar water, and the band at 1,630 cm^{-1} is due to the δ-HOH vibration [16, 19–21].

For the fresh catalyst, the existence of IR bands at 1,215, 1,135, 1,086, and 997 cm^{-1} can be attributed to S=O and S–O asymmetric and symmetric vibrations, which confirms

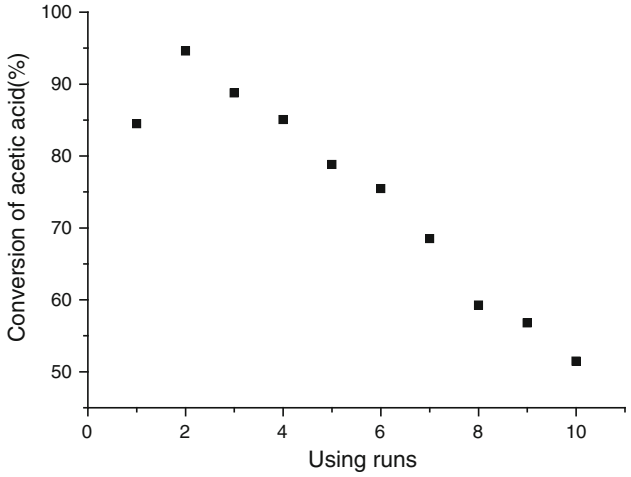

Fig. 1 Stability of sulfate-promoted iron oxide

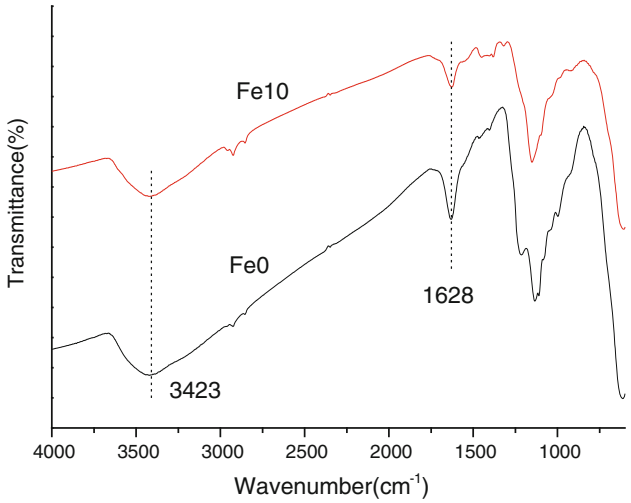

Fig. 2 IR patterns of Fe0 and Fe10 from 4,000 to 600 cm^{-1}

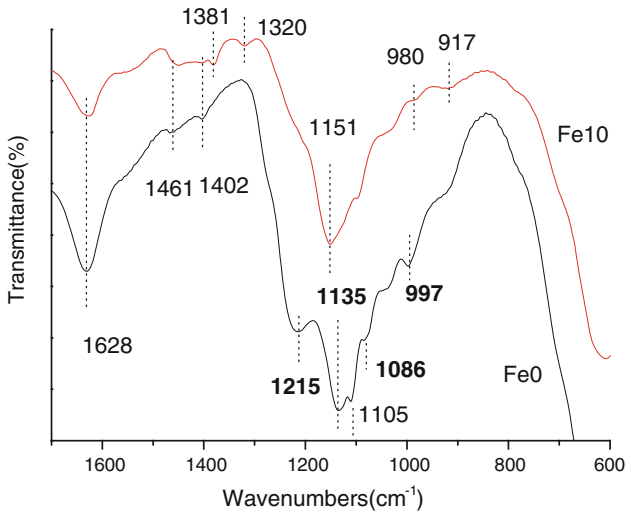

Fig. 3 IR patterns of Fe0 and Fe10 from 1,700 to 600 cm^{-1}

that chelated or bridged bidentate sulfate groups have been combined on the Fe_2O_3. The chelated or bridged bidentate sulfate groups are considered to be common active sites on the sulfate-promoted oxidized samples [1].The bands at 1,461, 1,402 cm^{-1} can be due to water adsorbed on the catalyst [16]. Additionally, the bands at 1105 cm^{-1} can be attributed to the existence of a small amount of free sulfate groups with Td symmetry [20].

For the deactivated catalyst, the bands at 1,381, 1,320, 1,151, 980, 917 cm^{-1} can be attributed to organic sulfate esters (O=S=O) $(OR)_2$ [1]. Yamaguchi [1] points out organic sulfate esters (O=S=O) $(OR)_2$ characteristic IR bands are [1,350–1,460, 1150–1,230, 975–1,000 cm^{-1}] (for ν_3), and 910 cm^{-1} (for ν_1). The bands in the region of 1461–1,402 cm^{-1} may be due to water and organic sulfate esters adsorbed on the deactivated catalyst [1, 16, 20], also supporting the existence of organic sulfate esters (O=S=O) $(OR)_2$ [R=C_4H_9].

Due to the observable existence of the organic sulfate esters in IR bands of the deactivated catalyst, a possible deactivation mechanism for sulfate-promoted iron oxide is proposed in Scheme 1.

The above scheme is actually showing that originally strong Lewis-acidic Fe^{3+} cations, to which surface sulfate groups coordinated, can be hydrolyzed by H_2O and alcoholyzed by *n*-butanol, so turning surface sulfate groups into sulfate esters and turning strong Lewis-acidic metal Fe^{3+} cations into weak Lewis-acidic Fe–OH moieties. The driving force for the hydrolysis and alcoholysis may be that the iron oxide was hydrophilic and tend to combine with hydroxyl groups from the *n*-butanol and produced water. In the mechanism, the main deactivating steps are: (1) Fe–O–(SO_2)–O–Fe moieties, including sulfate groups coordinated to Fe^{3+} cations, are turned into Fe–OH and Fe–O–(SO_2)–O–C_4H_9 and even C_4H_9–O–(SO_2)–O–C_4H_9 after Fe^{3+} cations' alcoholysis by *n*-butanol. (2) Fe–O–(SO_2)–O–Fe moieties are turned into Fe–OH and Fe–O–(SO_2)–OH after Fe^{3+} cations' hydrolysis by H_2O. Subsequently, Fe–O–(SO_2)–OH can be turned into Fe–O–(SO_2)–O–C_4H_9 and even C_4H_9–O–(SO_2)–O–C_4H_9 by *n*-butanol. Certainly, Fe–O–(SO_2)–OH can also be turned into free sulfate groups after Fe^{3+} cations' hydrolysis by H_2O. So, the surface sulfate groups, originally coordinated to Fe^{3+} cations, may be turned into free sulfate groups and organic sulfate esters as Fe–O–(SO_2)–O–C_4H_9 and C_4H_9–O–(SO_2)–O–C_4H_9.

Emphatically, in the proposed mechanism by us, the water produced from the esterification may play a key role on the deactivation, because it can directly hydrolyze strong Lewis- acidic Fe^{3+} cations of the catalyst to form weak Lewis-acidic Fe–OH species and so turn surface sulfate groups into free sulfate groups, and simultaneously it also can accelerate and facilitate the alcoholysis of strong Lewis-acidic Fe^{3+} cations of the catalyst to form weak Lewis-acidic Fe–OH species, turning surface sulfate groups into sulfate esters.

Based on the proposed mechanism, with a continual use of the sulfated iron oxide, more and more Fe^{3+} cations of strong Lewis acidity may turn into Fe–OH moieties of weak Lewis acidity which can not generate strong Bronsted acidity of the catalyst any more [1]. Simultaneously, more and more surface sulfate groups are transformed into free sulfate groups and sulfate esters. The originally strong coordination between Fe^{3+} cations and surface sulfate groups, which can induce and generate strong Lewis acidity of Fe^{3+} cations [1], is destructed, so leading to the acidity degradation of the catalyst, and so finally leading to the gradual deactivation of it in the esterification.

Additionally, the produced organic sulfate esters are generally weakly-physisorbed on the catalysts, but some of them may be chemically-adsorbed onto other strong Lewis-acidic Fe^{3+} cations and/or Bronsted acidic sites generated by strong Lewis-acidic Fe^{3+} cations, and may be subsequently turned into 1-butene and 2-butene (seen in Scheme 1) and other side products [21], which may progressively accelerate the deactivation of the catalyst.

Farcasiu et al. [21] confirmed the existence of surface sulfate esters appearing on sulfate-promoted zirconia during the conversion of benzene, and Suwannakarn et al. [22] also confirmed the existence of surface sulfate esters appearing on sulfate-promoted zirconia during the transesterification of triglycerides. These researches results [21, 22] support the above deactivation mechanism proposed by us. Additionally, Farcasiu et al. [21] proposed an oxidizing mechanism of reactions of alkanes on sulfate-promoted zirconia, thinking that the high activity of sulfate-promoted metal oxides in alkane conversion is due to their one-electron oxidizing ability, leading to ion-radicals and then to surface sulfate esters, which are the active intermediates in the mechanism. These surface sulfate esters either ionize generating carbocations or eliminate forming olefins, both by carbocationic reactions with no requirement of superacidity.

Based on the paper of Suwannakarn et al. [22], some other workers consider that water can wash away catalysts' surface sulfate groups. As reported previously, ionic sulfur groups supported on the sulfate-promoted zirconia catalyst surface can be modified and successively transformed into H_2SO_4, HSO_4^-, and SO_4^{2-} by the presence of free water in the liquid phase, leading to the loss of active sites from the solid surface. Omota et al. [22], for instance, reported that after contacting fresh sulfate-promoted zirconia catalyst samples with water, a rapid drop in the pH of the solution occurred, indicating that acid groups likely were being leached out into solution. Other authors [22] also have documented water's capability of leaching out the active catalytic groups in SZ. In the deactivation mechanism

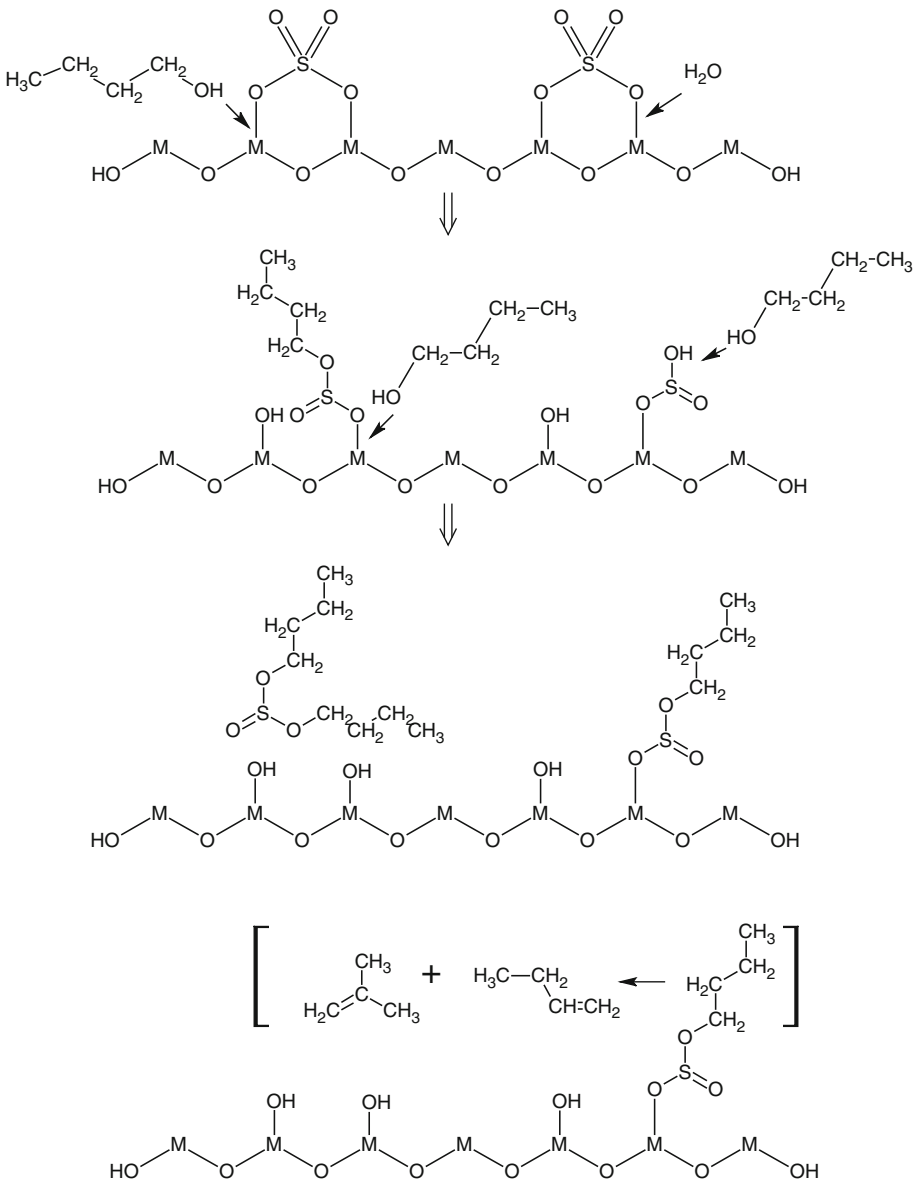

Scheme 1 A proposed deactivation mechanism for sulfate-promoted iron oxide (*M* stands for Fe)

proposed by us, the originally strong coordination between surface sulfate groups and Fe^{3+} cations can be destructed by Fe^{3+} cations' hydrolysis by H_2O, and so some surface sulfate groups are turned into free sulfate groups, corresponding to these authors' viewpoints.

Suwannakarn et al. [22] think alcohols can also wash away catalysts' surface sulfate groups despite of a by far weaker washing functionality of them than that of water. Suwannakarn et al. observed monoalkyl hydrogen sulfate and dialkyl sulfate in the methanol filtrate solution after washing sulfate-promoted zirconia by ^1H NMR studies, and deduced that the removal of sulfate ions from the catalyst surface as sulfuric acid in alcohols(methanol, ethanol, and butanol), which subsequently reacts with alcohol to form monoalkyl hydrogen sulfate and dialkyl sulfate. In the deactivation mechanism proposed by us, the originally strong coordination between surface sulfate groups and Fe^{3+} cations can be destructed by Fe^{3+} cations' alcoholysis by *n*-butanol, and so some surface sulfate groups are turned into sulfate esters, corresponding to these authors' viewpoints.

In all, the deactivation mechanism proposed by us, supported by our IR results and some other authors' researches [21], [22] can interpret well the deactivation process of the catalyst in the esterification.

3.3 XRD Patterns of the Catalysts

The XRD patterns of the new and the deactivated catalysts and their precipitate counterpart are presented in Fig. 4. The iron hydroxide precipitate is amorphous. The most important characteristic lines of the two diffractograms of

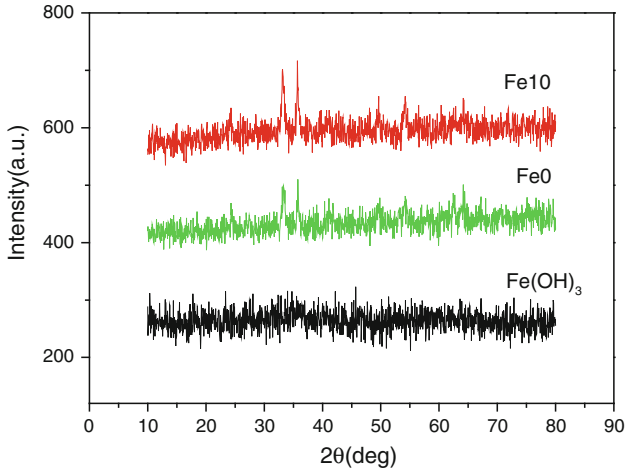

Fig. 4 XRD patterns of Fe $(OH)_3$, Fe0 and Fe10

sulfate-promoted iron oxides catalysts (the new and deactivated) are observed at 33° and 35°, showing clearly that the hematite phase dominates in the iron oxide [19]. Obviously, the deactivated catalyst has a larger crystallinity than the new one, indicating a continual transformation from the amorphous phase to the hematite phase with the continual use of the sulfated iron oxide. Based on the above proposed deactivation mechanism of the sulfated iron oxide in the esterification, the originally strong coordination between surface sulfate groups and Fe^{3+} cations can be destructed by Fe^{3+} cations' hydrolysis by H_2O and Fe^{3+} cations' alcoholysis by *n*-butanol, and the sulfate groups are transformed into free sulfate groups and sulfate esters. The free sulfate groups can enter into the reaction liquid mixture and can be further turned into sulfate esters, and the unwanted sulfate esters are generally weakly physisorbed on the surface of the catalyst. So, they can not effectively slow the phase transformation from the amorphous phase to the hematite phase any more [1]. Therefore, the proposed deactivation mechanism can interpret well the increased crystallinity of the deactivated catalysts.

3.4 Specific Surface Areas and Pore Distributions of the Catalysts

Specific surface area and pore structural parameters of the catalysts are shown in Table 1.

The isotherms obtained for Fe0 and Fe10 are both ones of type IV (seen in Fig. 5). This type of isotherm indicates, unequivocally, the presence of a lot of mesopores in the sulfate-promoted samples.

The specific surface area of the deactivated catalyst is 62.95 m^2/g, smaller than 73.42 m^2/g of the fresh catalyst. During the esterification, the sulfate groups, originally coordinated to Fe^{3+} cations, transformed into free sulfate groups and sulfate esters based on the proposed deactivation mechanism as before, facilitating the crystallization of the catalyst so as to decrease the specific surface area of the deactivated catalyst. The pore volume of the deactivated catalyst is smaller than the fresh one, which can also be discerned from Fig. 6 besides from Table 1, may be partly due to the produced sulfate esters' filling the inter-particle pores to some extent.

Table 1 Specific surface area and pore structural parameters of the catalysts

	Fe0	Fe10
Specific surface area (m^2/g)	73.42	62.95
Pore volume (cm^3/g)	0.247	0.173
The average pore diameter (nm)	13.58	13.42

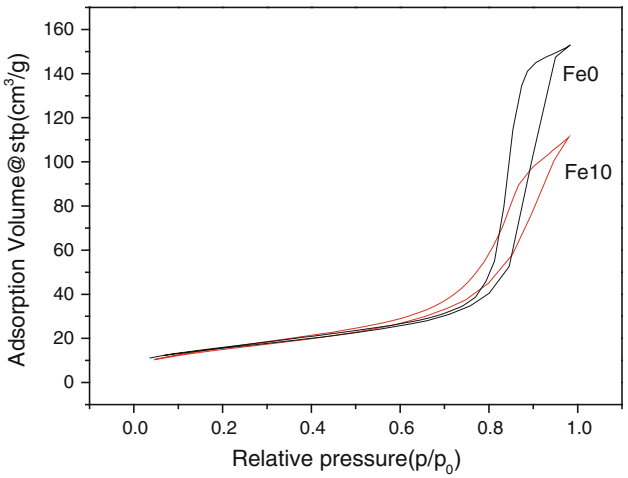

Fig. 5 N_2 adsorption/desorption isotherms for Fe0 and Fe10

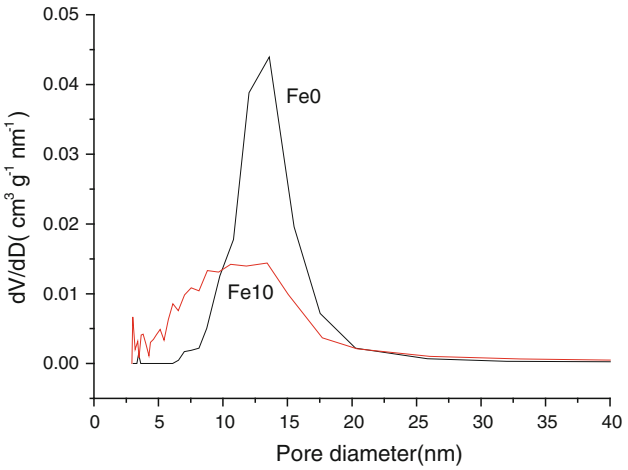

Fig. 6 Pore size distributions for Fe0 and Fe10

3.5 Thermal Analysis of the Catalysts

The TG profiles of the new and deactivated sulfate-promoted iron oxides are shown in Figs. 7, 8. Referenced to literatures [23], the TG and DSC profiles of the fresh and the deactivated catalysts are analyzed as below.

For the fresh catalyst, below 200 °C, the weight loss can be mainly attributed to the removal of water (in hydration or structural), an endothermic process seen in its DSC curve. In the region of 200–550 °C, the weight loss of the fresh sulfate-promoted iron oxide can be mainly attributed to dehydroxylation which is accompanied by phase transformation which are exothermic seen in its DSC curve; From around 550 °C on, there comes a gradual evolution of SO_x (SO_3, SO_2) due to sulfate groups' decomposition, which are endothermic seen in its DSC profile.

However, for the deactivated catalyst, below 500 °C, the weight loss can be partly attributed to the removal water and dehydroxylation, partly attributed to the decomposition of free sulfate groups leached from the catalyst, an apparent endothermic process seen in its DSC curve, which are accompanied by phase transformation. Emphatically, the decomposition of free sulfate groups leached from the catalyst under a relatively-low temperature below 500 °C, supporting the proposed deactivation mechanism as before. From around 500 °C on, there comes an almost-indiscernible gradual evolution of SO_x (SO_3, SO_2) due to sulfate groups' decomposition, which is weakly endothermic seen in DSC profiles of the fresh and the deactivated sulfate-promoted iron oxides, disclosing a smaller amount of surface sulfate groups content on the deactivated catalyst than that on the fresh one.

Based on the above TG analyses, the estimated sulfate groups' contents are 5.00 wt% for the new and 4.00 wt% for the deactivated catalyst, respectively. Therefore, a surface sulfate groups' loss of 1 wt% comes on the deactivated sample. On the deactivated mechanism proposed by us, surface sulfate groups' loss is arisen from free sulfate groups leached from the catalyst, which are labile and easy to decompose into H_2O and O_2 and SO_2 under a relatively-low temperature below 500 °C. Emphatically, in the region of 450–550 °C, a gradual and slow decreasing of weight loss is seen for the new, but a platform appears for the deactivated sample, which may be due to the absence of the surface sulfate groups which have already be lost as free sulfate groups, supporting the proposed deactivation mechanism as before.

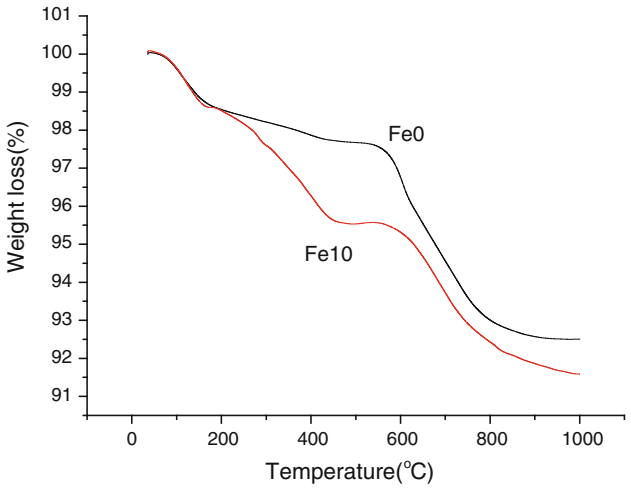

Fig. 7 TG profiles for Fe0 and Fe10

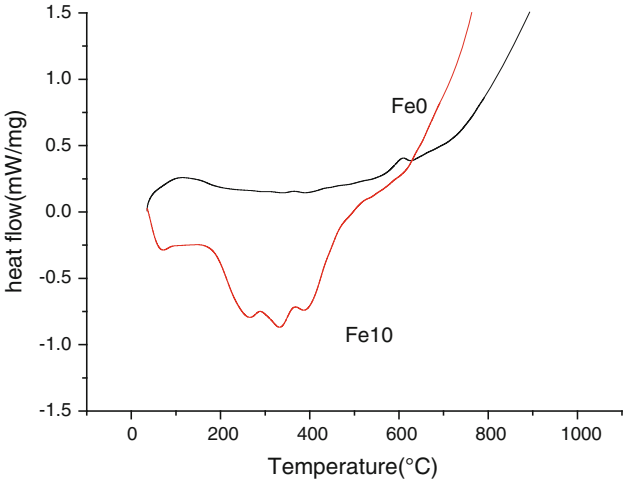

Fig. 8 DSC profiles for Fe0 and Fe10

Emphatically, the remaining 4.00 wt% sulfate groups still stand on the deactivated catalyst, but they may be turned into sulfate esters based on the proposed deactivation mechanism of the catalyst in the esterification. The originally strong-and-catalytic Lewis-acidic Fe^{3+} cations are rehydroxylated to form Fe–OH moieties of weak Lewis acidity, not to generate strong Bronsted acid sites any more. The type of acidity degradation of the catalyst leads to the considerable deactivation of it.

3.5.1 SEM Photos of the Catalysts

The deactivated catalyst (Fig. 9) has smaller particle diameters and less aggregation than the new one (Fig. 10). The results are also be partly interpreted by the proposed deactivation mechanism as before. Because that surface sulfate groups and Fe^{3+} cations are continually hydrolyzed and alcoholyzed by H_2O and *n*-butanol, sulfate groups are turned into free sulfate groups and sulfate esters, and so originally strong Fe–S–O linkages are destructed, so as to make originally larger-in-diameter particles suffer from surface segregation and split into many smaller-in-diameter particles.

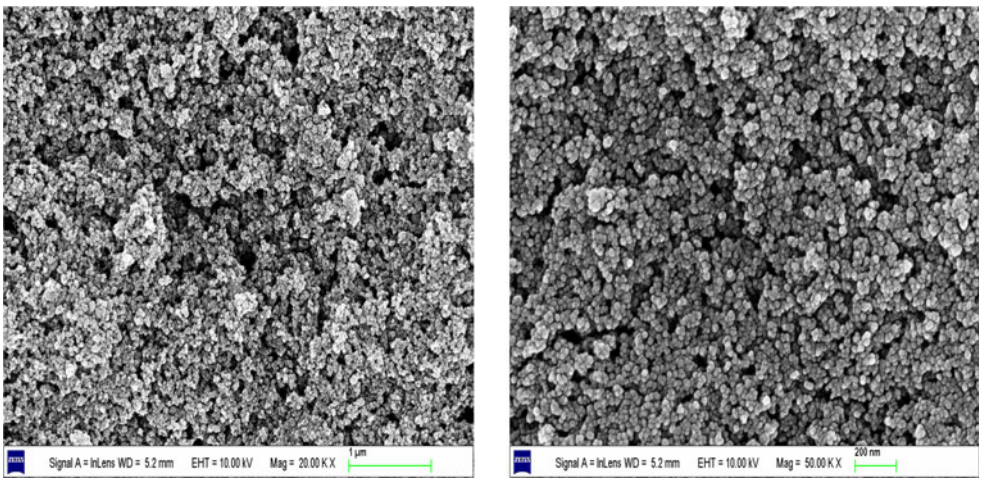

Fig. 9 SEM photos of Fe10

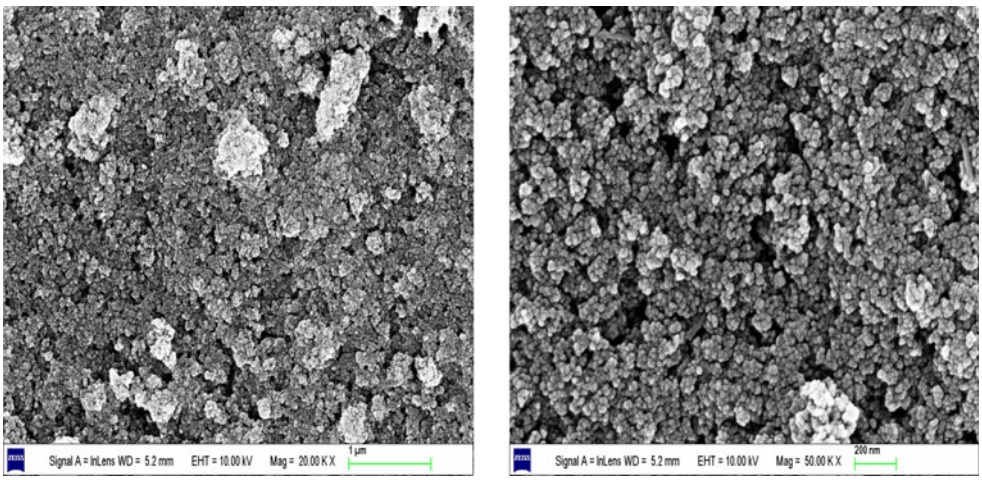

Fig. 10 SEM photos of Fe0

3.5.2 NH_3–TPD Curves of the Catalysts

The acidity of the catalysts was measured by NH_3–TPD. The TPD profiles of desorbed ammonia (NH_3) on the fresh and the deactivated catalysts are shown in Fig. 11.

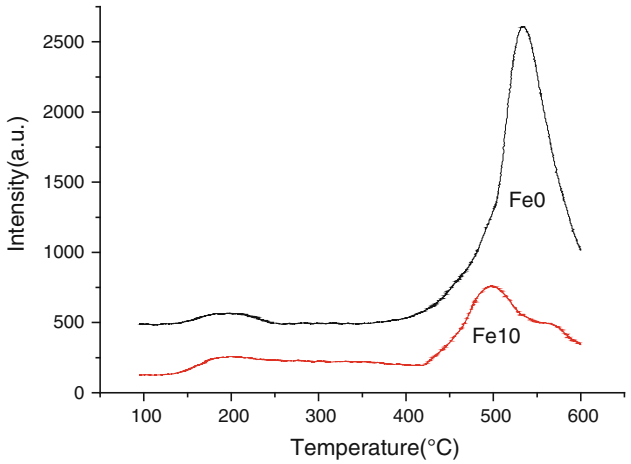

Fig. 11 NH_3–TPD profiles for Fe0 and Fe10

Referenced to literatures [24, 25], the NH_3–TPD profiles of the fresh and the deactivated catalysts are analyzed as below. For the fresh catalyst, a lower temperature (~200 °C) NH_3 desorption broad peak is attributed to weak acid sites, whereas the higher temperature (~535 °C) NH_3 desorption peak is attributed to very strong acid sites. For the deactivated catalyst, a lower temperature (~200 °C) NH_3 desorption broad peak is attributed to weak acid sites, and the NH_3 desorption peak at around 499 °C is attributed to very strong acid sites. The above results show that the fresh catalyst is stronger in acid strength than the deactivated one. Besides, the surface acidic active sites on the deactivated sulfate-promoted iron oxide decrease its concentration considerably, only about one-third of that on the fresh sulfate-promoted iron oxide, which is estimated by the integral areas of NH_3 desorption curves of the new and the deactivated catalysts. Based on the proposed deactivation mechanism of sulfated iron oxide, surface sulfate groups originally coordinated to Fe^{3+} cations are turned into free sulfate groups and sulfate esters, the acidity degradation of the catalyst is bound to take place, because the originally strong coordination between Fe^{3+} cations and surface sulfate groups

is destructed, and originally strong Lewis-acidic Fe^{3+} cations, induced and generated by surface sulfate groups, are hydrolyzed or alcoholyzed into weak Lewis-acidic Fe–OH moieties, which can also not generate strong Bronsted acidity any more.

4 Conclusions

(1) IR results disclose that surface groups which originally coordinated to Fe^{3+} cations may be turned into free sulfate groups and even sulfate esters

(2) Based on IR results, a possible deactivation mechanism is put out tentatively. Namely, surface sulfate groups, which are originally coordinated to Fe^{3+} cations and can so induce and generate strong Lewis acidity of Fe^{3+} cations, may have been gradually turned into free sulfate groups and sulfate esters, arisen from strong Lewis-acidic Fe^{3+} cations' being hydrolyzed by H_2O and their being alcoholyzed by *n*-butanol, which leads to a gradual destruction of the originally strong coordination between Fe^{3+} cations and surface sulfate groups, so leading to the acidity degradation of the catalyst, and finally leading to the deactivation of it. Emphatically, in the proposed mechanism, the water produced from the esterification may play a key role in the deactivation of the catalyst, because it can directly hydrolyze some strong Lewis-acidic Fe^{3+} cations of the catalyst and indirectly promote the alcoholysis of them, to form weak Lewis-acidic Fe–OH species.

(3) The deactivated catalyst has a larger crystallinity, a smaller specific surface area, a smaller sulfate groups content, a weaker acidity than the fresh. All the phenomena, accompanying the deactivation of sulfate-promoted iron oxide, can be interpreted by the proposed deactivation mechanism very well.

References

1. Yamaguchi T (1990) Recent progress in solid superacid. Appl Catal 61:1–25
2. Yamaguchi T (2001) Alkane isomerization and acidity assessment on sulfated ZrO_2. Appl Catal A-Gen 222:237–246
3. Reddy BM, Patil MK (2009) Organic syntheses and transformations catalyzed by sulfated zirconia. Chem Rev 109:2185–2208
4. Huang YY, Timothy JM, Wolfgang MH (1996) Preparation and catalytic testing of mesoporous sulfated zirconium dioxide with partially tetragonal wall structure. Appl Catal A-Gen 148: 135–154
5. Mantilla A, Ferrat G, López-Ortega A, Romero E, Tzompantzi F, Torres M, Ortíz-Islas E, Gómez R (2005) Catalytic behavior of sulfated TiO_2 in light olefins oligomerization. J Mol Catal A-Chem 228:333
6. Ma Z, Yue YH, Deng XY, Gao Zi (2002) Nanosized anatase TiO_2 as precursor for preparation of sulfated titania catalysts. J Mol Catal A-Chem 178:97–104
7. Das D, Mishra HK, Dalai AK, Parida KM (2003) Isopropylation of benzene over sulfated ZrO_2–TiO_2 mixed-oxide catalyst. Appl Catal A-Gen 243:271–284
8. Colón G, Hidalgo MC, Navío JA, Kubacka A, Fernández-García M (2009) Influence of sulfur on the structural, surface properties and photocatalytic activity of sulfated TiO_2. Appl Catal B-Environ 90:633–641
9. Satoh K, Matsuhashi H, Arata K (1999) Alkylation to form trimethylpentanes from isobutane and 1-butene catalyzed by solid superacids of sulfated metal oxides. Appl Catal A-Gen 189:35–43
10. Das SK, Bhunia MK, Sinha AK, Bhaumik A (2009) Self-assembled mesoporous zirconia and sulfated zirconia nanoparticles synthesized by triblock copolymer as template. J Phys Chem C 113:8918–8923
11. Wang SN, Matsumura S, Toshima K (2007) Sulfated zirconia (SO_4/ZrO_2) as a reusable solid acid catalyst for the Mannich-type reaction between ketene silyl acetals and aldimines. Tetrahedron Lett 48:6449–6452
12. Ma HZ, Xiao J, Wang B (2009) Environmentally friendly efficient coupling of *n*-heptane by sulfated tri-component metal oxides in slurry bubble column reactor. J Hazard Mater 166:860–865
13. Mao W, Ma HZ, Wang B (2010) Mild ring-opening coupling of liquid-phase cyclohexane to diesel components using sulfated metal oxides. J Hazard Mater 176:361–366
14. Sunajadevi KR, Sugunan S (2006) Selective nitration of phenol over sulfated Titania systems prepared via sol-gel route. Mater Lett 60:3813–3817
15. Sohn JR, Lee SH, Lim JS (2006) New solid superacid catalyst prepared by doping ZrO_2 with Ce and modifying with sulfate and its catalytic activity for acid catalysis. Catal Today 116:143–150
16. Miao CX, HUA WM, Chen JM, GAO Z (1996) Sulfated binary and trinary oxide solid superacids. Sci China Ser B-Chem 39:406–415
17. Li BH, Richard DG (1998) An in situ DRIFTS study of the deactivation and regeneration of sulfated zirconia. Catal Today 46:55–67
18. Fogash KB, Hong Z, Kobe JM (1998) Deactivation of sulfated-zirconia and H-mordenite catalysts during *n*-butane and isobutane isomerization. App. Catal A-Gen 172:107–116
19. Kang ZJ, Ma HZ, Wang B (2009) Removal of thiophene from coking benzene over SO_4^{2-}/Fe_2O_3 solid acid under mild conditions. Ind Eng Chem Res 48:9346–9349
20. Wang ZC, Hu XF, Käll PO, Helmersson U (2001) High Li^+-ion storage capacity and double-electrochromic behavior of sol−gel-derived iron oxide thin films with sulfate residues. Chem Mater 3:1976–1983
21. Farcasiu D, Ghenciu A (1996) The mechanism of conversion of hydrocarbons on sulfated metal oxides. Part II. Reaction of benzene on sulfated zirconia[J]. J Mol Catal A: Chem 109:273–283
22. Suwannakarn K, Lotero E, Goodwin JG Jr, Lu CQ (2008) Stability of sulfated zirconia and the nature of the catalytically active species in the transesterification of triglycerides. J Catal 255:279–286
23. Noda LK, Gonçalves NS, de Borba SM, Silveira JA (2007) Raman spectroscopy and thermal analysis of sulfated ZrO_2 prepared by two synthesis routes. Vib Spectrosc 44:101-107
24. Jong RS, Jong-Geol K, Tae-Dong K, Hee PE (2002) Characterization of titanium sulfate supported on zirconia and activity for acid catalysis. Langmuir 18:1666-1673
25. Srinivasan R, Keogh RA, Davis BH (1995) Activation and characterization of Fe–Mn–SO_4^{2-}/ZrO_2 catalysts. Appl Cat A: General 130:135-155